YALE
PEABODY
MUSEUM

JOURNAL OF MARINE RESEARCH

The *Journal of Marine Research,* one of the oldest journals in American marine science, published important peer-reviewed original research on a broad array of topics in physical, biological, and chemical oceanography vital to the academic oceanographic community in the long and rich tradition of the Sears Foundation for Marine Research at Yale University.

An archive of all issues from 1937 to 2021 (Volume 1–79) are available through EliScholar, a digital platform for scholarly publishing provided by Yale University Library at https://elischolar.library.yale.edu/.

Requests for permission to clear rights for use of this content should be directed to the authors, their estates, or other representatives. The *Journal of Marine Research* has no contact information beyond the affiliations listed in the published articles. We ask that you provide attribution to the *Journal of Marine Research.*

Yale University provides access to these materials for educational and research purposes only. Copyright or other proprietary rights to content contained in this document may be held by individuals or entities other than, or in addition to, Yale University. You are solely responsible for determining the ownership of the copyright, and for obtaining permission for your intended use. Yale University makes no warranty that your distribution, reproduction, or other use of these materials will not infringe the rights of third parties.

Diffraction and refraction calculations for waves incident on an island

by Ivar G. Jonsson[1], Ove Skovgaard[1] and Ole Brink-Kjaer[2]

ABSTRACT

An island of circular cylindrical shape, situated on a paraboloidal shoal (Fig. 1 and Table 1) in an infinite ocean of constant depth is attacked by small regular waves of long period and of plane incidence. The wave field around the island is calculated according to two different approaches, viz. a diffraction theory and a refraction theory (i.e. geometrical optics). The solutions are compared for those (tsunami) periods, where the Coriolis force can be neglected. It is found that in a certain range, the refraction solution can predict the critical wave periods quite well, and to some extent also the regions of the shoreline where the wave amplitude is large. For L_a smaller than (say) 0.4 r_a (L_a is the wave length at the shoreline, and r_a the island radius) the amplitudes at the middle of the front face of the island are rather well predicted by the primary orthogonal. However, this cannot predict the critical wave periods, nor the more exposed shoreline regions, but up to $L_a \approx 2.5 \ r_a$ it can give the right order of magnitude of the amplitudes, in the sense that it gives an approximation to an amplitude versus period diffraction curve, where the undulations are smoothed out. For L_a larger than about 2.5 r_a both the primary orthogonal and the complete refraction solution give quite absurd results.

The conflicting data in the definition of a similar island by Vastano and Reid (1966, 1967) are clarified. For another set of data the diffraction solution is given with a more complete description of the wave field over the shoal, and two test solutions are tabulated (Table 2). For the first time, the diffraction solution is given for an island of this form using intermediate depth theory and a newly introduced mild-slope wave equation.

1. Introduction

When a tsunami (typical period 5-60 min) reaches an island it is often drastically amplified due to the sea bed topography, and at the coast this is a highly nonlinear phenomenon. As formulated by Smith and Sprinks (1975): "Although tsunamis are dramatically nonlinear in their final run-up with amplitudes as high as 10 m, out at sea their amplitudes are considerably smaller and it is reasonable to assume that the topographic modification prior to run-up can be accurately described by linear-

1. Institute of Hydrodynamics and Hydraulic Engineering (ISVA), Technical University of Denmark, Building 115, DK-2800 Lyngby, Denmark.
2. Present address: Computational Hydraulics Centre, Danish Hydraulic Institute, DK-2970 Hørsholm, Denmark.
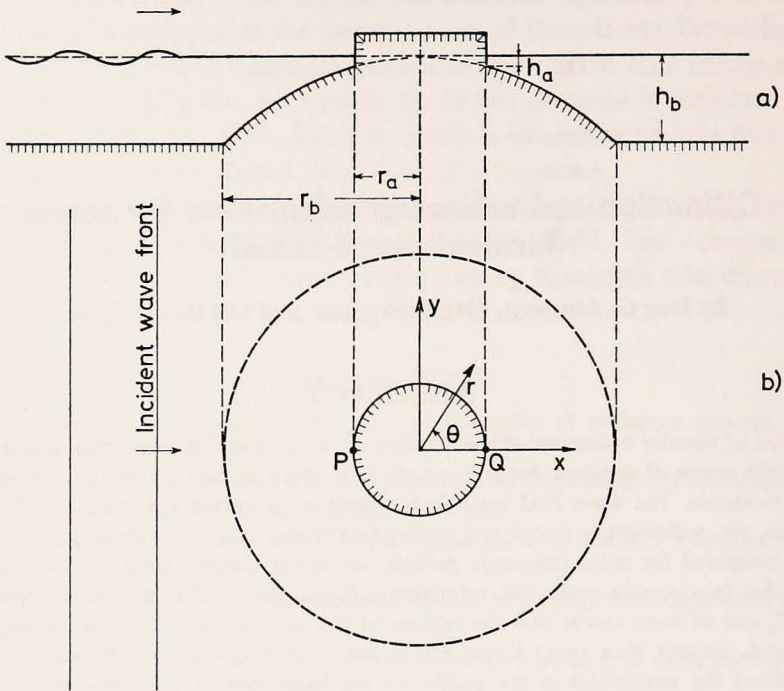
Figure 1. Sketch of the idealized island on a paraboloidal shoal with $h = \alpha r^2$; (a) vertical,
(b) horizontal.

ized equations." In accordance with this, both the refraction theory and the diffrac-
tion theory, which are used below to describe the wave field near the coast, are
based on linearized equations.

In the last decade a number of computer programs have been developed for the
calculation of depth refraction; see the survey in Skovgaard et al. (1975, 1976).
From the point of view of economy and numerical accuracy these programs have
today reached a satisfactory level. Within a few years we will no doubt also see
many computer programs which will account for diffraction of water waves over
a varying sea bed, i.e. diffraction in an inhomogeneous medium. Initial steps in this
direction, based on finite element methods, have been taken by Berkhoff (1973,
1975) and by Chen and Mei (1974). These programs, which essentially solve a
boundary value problem (the reduced wave equation) or the equivalent variational
formulation, are not yet developed for general use and are today much more ex-
pensive to use than refraction programs which solve an initial value problem.
Therefore both approaches will be used in the coming years, although as this paper
demonstrates, the latter has severe limitations. (In this connection it should be re-
marked that Berkhoff, although he presented a fundamentally new wave equation,

Table 1. Geometrical data for island and paraboloidal shoal.

Shoreline radius r_a . . . . 10,000 m
Outer radius of shoal . . . . 30,000 m
Depth h_b . . . . 4,000 m
Shoreline depth $h_a = h_b \, (r_a/r_b)^2 = 4,000/9 \approx 444$ m

did not use a correct functional (Berkhoff (1973), p. 478 and (1975), p. 255), as pointed out by Chen and Mei (1974).)

The physical limitations of refraction programs are seldom discussed. A major problem is: How (in)accurate is a refraction solution when there are large variations in depth over one wave length? The best way to study this effect is to make a comparison between wave amplitudes calculated on the basis of simple refraction theory and those emerging from the complete solution of the reduced wave equation (diffraction). Another problem is that the presence of structures, peninsulas and islands, yields areas of "geometrical shadow" which indicate that the refraction theory is insufficient.

In this paper we shall study an idealized island of circular cylindrical shape situated on a paraboloidal shoal (Fig. 1 and Table 1) in an infinite ocean of constant depth, attacked by small, monochromatic, plane, incident waves. The water depth h is

$$h = \alpha r^2 \qquad \text{for } r_a \leq r \leq r_b \qquad \text{and } 0° \leq \theta < 360°$$

(1.1)

$$h = h_b \, (= \alpha r^2_b) \text{ for } r_b \leq r < +\infty \quad \text{and } 0° \leq \theta < 360°$$

where the factor of proportionality α for the data in Table 1 becomes $\alpha = 4,000/30,000^2 = 4/9 \times 10^{-5}$ m^{-1}. Subscript a denotes values at the shoreline and subscript b denotes values at the outer boundary of the shoal.

This type of island is seemingly accepted as being representative for some real cases (Homma, 1950; Vastano and Reid, 1966 and 1967). A discussion of tsunami amplification over other depth profiles is given by Meyer (1971).

In the shallow water approach the paraboloidal shape of the shoal acts as a special "wave guide", since here the phase velocity is proportional to distance from the center of the island, see Section 4.a.

The purpose of the paper is threefold. First and foremost we will present an intermediate depth diffraction solution in detail and compare it with the shallow water diffraction solution. We hope that this will be useful for those who work on general numerical schemes for diffraction problems. Second, we will present the refraction solution, attaching the greatest importance to qualitative considerations. Third, we will present the results of a comparison between the diffraction and refraction solutions, and so demonstrate that a refraction calculation is quite meaningless in a wide range.

The wave field around an island similar in shape to the one in Fig. 1 was first investigated in the pioneer works by Homma (1950), and Vastano and Reid (1966, 1967). Homma presented the analytical solution to the shallow water wave equation for the island in Fig. 1 for plane wave incidence. He also took steps to calculate a refraction solution. Since the differential equation for the wave separation factor was not published until two years later (Munk and Arthur, 1952), and since electronic computers were not available at that time, only a few numerical results could be presented in broad outline. Furthermore, these calculations are inaccurate as regards the wave amplitude. Pure depth refraction of surface gravity waves about circular islands was first studied by Arthur (1946) and Pocinski (1950).

In the short-wave limit (here the wave length is compared with horizontal scales, not depths) Keller's geometrical diffraction theory (see Keller, 1962; Christiansen, 1975; and Larsen and Christiansen, 1975) presents an alternative to the finite element methods. Keller's theory, the so-called ray (tracing) method, is especially advantageous when the boundaries are but weakly reflecting.

The problem of scattering due to a transient wave motion has been considered by Shaw (1975).

2. Assumptions

The incoming waves are assumed plane, monochromatic, irrotational, and of small amplitude. There are no currents. The Coriolis force is neglected, so we assume tsunami periods T smaller than (say) 30 min. The spherical form of our planet is also neglected.

All governing equations for both a diffraction and a refraction approach are given for the intermediate depth dispersion relation

$$c = \sqrt{\frac{g}{k} \tanh kh} \qquad (2.1)$$

where k is the wave number $2\pi/L$, L $(= cT)$ is the wave length, c is the phase velocity, and g is the gravity acceleration. In addition to the numerical solutions of the equations with the dispersion relation (2.1), the equations are solved analytically, using the shallow water relation

$$c = \sqrt{gh} \qquad (2.2)$$

Disintegration into minor waves of shorter period is neglected. If the bottom is steep, this assumption is questionable for long waves of appreciable height. Such waves show a tendency to be unstable in this sense under shoaling conditions; see e.g. Madsen and Mei (1969).

Bottom friction and other dissipative mechanisms are disregarded. The Danish Refraction Program (Skovgaard and Bertelsen, 1974, and Skovgaard *et al.*, 1975, 1976) can include this effect.

It was excluded from the present study, however, since it is not contained in the diffraction solutions. Furthermore, the bottom friction model was based on waves of rather short period, i.e. where the wave boundary layer is thin as compared with the depth (see Jonsson, 1967, 1975, 1976, and Jonsson and Carlsen, 1976). Frictional coefficients for long-period waves, on the other hand, were calculated by Kajiura (1964).

So, summing up, it can be stated that all nonlinear effects are neglected.

Only one island is examined; see Fig. 1 and Table 1. The incident wave orthogonals are propagating in the direction of the positive x-axis. The vertical sides of the island are assumed fully reflecting.

In the refraction approach, energy transport across the "geometrical optics orthogonals" is excluded.

Let it be stressed for completeness that our use of the word refraction is different from that of Lautenbacher (1970) who uses the word refraction for what we call diffraction (over a varying bottom).

3. The diffraction solution

Rewriting Berkhoff's linear two-dimensional differential equation (Berkhoff, 1973, Eq. 20) for the calculation of the combined effects of refraction and diffraction for a simple harmonic surface gravity wave motion over a water area of gradually varying depth, Jonsson and Brink-Kjaer (1973) introduced the following reduced mild-slope wave equation

$$\nabla \cdot (c\, c_g \nabla \eta) + \frac{c_g}{c}\, \omega^2 \eta = 0 \ . \tag{3.1}$$

In this expression ∇ is the horizontal gradient operator $(\partial/\partial x, \partial/\partial y)$ or $(\partial/\partial r, r^{-1} \partial/\partial \theta)$, c_g is the group velocity

$$c_g = \tfrac{1}{2}\, c\, (1 + G) \tag{3.2}$$

where

$$G \equiv \frac{2kh}{\sinh\ 2kh} \tag{3.3}$$

$\eta = \eta(x,y)$ or $\eta(r,\theta)$ is the complex wave amplitude, and $\omega(= 2\pi/T)$ is the angular frequency. Note: The instantaneous elevation of the water surface is $\eta \exp(- i\omega t)$, i being the imaginary unit and t the time.[3] It also was shown by Jonsson and Brink-Kjaer (1973) that the one-dimensional version of (3.1) in fact is identical with the wave equation derived by Svendsen (1967), which confirms that (3.1) is correct to the first order in both wave amplitude and bottom slope. A full report is being prepared by Svendsen and Jonsson (1976). Using rather intuitive arguments, Smith and Sprinks (1975) independently proposed (3.1), but they only solved the well-known long-wave version of (3.1), see (3.18).

3. The letter i is used as subscript and as $\sqrt{-1}$.

In order to calculate the wave field we must solve the partial differential equation (3.1).

The wave field outside the shoal is composed of two parts, viz. the incident wave field η_i and the scattered wave field η_{sc}. Both η_i and η_{sc} satisfy (3.1), separately. This equation reads in polar co-ordinates on the constant water depth h_b

$$r^2 \frac{\partial^2 \eta}{\partial r^2} + r \frac{\partial \eta}{\partial r} + k^2_b r^2 \eta + \frac{\partial^2 \eta}{\partial \theta^2} = 0 \tag{3.4}$$

where k_b $(= 2\pi/L_b)$ is the wave number corresponding to the constant depth. The plane incident wave field is (omitting the harmonic time variation)

$$\eta_i = A_i \exp(ik_b x) \quad \text{or} \quad \eta_i = A_i \sum_{n=0}^{\infty} \epsilon_n i^n J_n (k_b r)\cos(n\theta) \tag{3.5a,b}$$

substituting $x = r \cos \theta$ and expanding. A_i is the real amplitude, J_n is the Bessel function of nth order and first kind, and ϵ_n is the Neumann factor or the Jacobi symbol, i.e. $\epsilon_n = 1$ for $n = 0$ and $\epsilon_n = 2$ for $n \neq 0$. Using the method of separation of variables, (3.4) gives for the scattered wave field

$$\eta_{sc} = \sum_{n=0}^{\infty} C_n H_n^{(1)} (k_b r)\cos(n\theta) \tag{3.6}$$

where we have used the radiation condition for scattered waves, i.e. the scattered wave field must be outgoing (and so vanishing) for $r \rightarrow \infty$ (see Sommerfeld, 1964, p. 188ff.), and that the solution must have a period 2π in θ. $H_n^{(1)}(\equiv J_n + iY_n)$ is the Hankel function of the nth order and first kind, Y_n is the Bessel function of nth order and second kind, and C_n are integration constants.

For the wave field over the shoal, (3.1) reads in polar co-ordinates

$$r^2 \frac{\partial^2 \eta}{\partial r^2} + \frac{r}{1+G} \left[1 + 7G - \frac{4Gkh}{(1+G) \tanh kh} \right] \frac{\partial \eta}{\partial r} + k^2 r^2 \eta + \frac{\partial^2 \eta}{\partial \theta^2} = 0 \tag{3.7}$$

The method of separation of variables gives here

$$\eta = \sum_{n=0}^{\infty} R_n (r)\cos(n\theta) \tag{3.8}$$

where $R_n(r)$ $(n = 0,1,2, \ldots)$ is the solution to the following linear ordinary differential equation

$$r^2 \frac{d^2 R_n}{dr^2} + \frac{r}{1+G} \left[1 + 7G - \frac{4Gkh}{(1+G) \tanh kh} \right] \frac{dR_n}{dr} + [k^2 r^2 - n^2] R_n = 0 \tag{3.9}$$

where $r_a \leqq r \leqq r_b$. In order to determine C_n in (3.6) and to solve (3.9), we need three boundary conditions. At $r = r_a$ the island is fully reflecting, i.e.

$$\frac{\partial \eta}{\partial r} = 0 \tag{3.10}$$

or

$$\left[\frac{dR_n}{dr}\right] = 0 \qquad n = 0,1,2,\ldots \tag{3.11}$$

At $r = r_b$ we have the two remaining conditions, viz. continuity in η and in the first derivative of η with respect to r

$$\eta = \eta_i + \eta_{sc} \tag{3.12}$$

$$\frac{\partial \eta}{\partial r} = \frac{\partial \eta_i}{\partial r} + \frac{\partial \eta_{sc}}{\partial r} . \tag{3.13}$$

Inserting (3.5b), (3.6), and (3.8) in (3.12) and (3.13) gives two infinite sets of equations

$$(R_n)_{\ r=r_b} = A_i \epsilon_n i^n J_n(\tau) + C_n H_n(\tau) \qquad n = 0,1,2,\ldots \tag{3.14}$$

$$\left(\frac{dR_n}{dr}\right)_{r=r_b} = A_i \epsilon_n i^n k_b J'_n(\tau) + C_n k_b H'_n(\tau) \qquad n = 0,1,2,\ldots \tag{3.15}$$

where primes indicate derivatives with respect to the argument, $\tau \equiv r_b k_b$, and we have dropped the superscript (1) on H_n and its derivative. J'_n and H'_n are calculated according to standard formulae, see e.g. Olver (1964), equations 9.1.27-28.

From (3.14) and (3.15) we can eliminate C_n, and thereby get the second boundary condition for (3.9), (3.11) being the first,

$$-H_n(\tau)\left(\frac{dR_n}{dr}\right)_{r=r_b} + k_b H'_n(\tau)\,(R_n)_{\ r=r_b} = \frac{2}{\pi}\,\epsilon_n\,\frac{A_i}{r_b}\,i^{n+1} \qquad n = 0,1,2,\ldots \tag{3.16}$$

where we have used the Wronskian formulae, see e.g. Erdélyi *et al.* (1953), equation 7.11.29:

$$H_n(\tau)J'_n(\tau) - J_n(\tau)H'_n(\tau) = -\frac{2i}{\pi\tau} . \tag{3.17}$$

Before we in Section 3.b present a numerical solution of the diffraction problem using intermediate depth theory we will first present the analytic solution for shallow water.

a. The diffraction solution using shallow water theory. In shallow water, i.e. for h/L smaller than (say) 1/20, we can solve the diffraction problem analytically. In this case, c is given by (2.2), and $G = 1$. The reduced wave equation (3.1) becomes equal to the well-known linearized long-wave equation

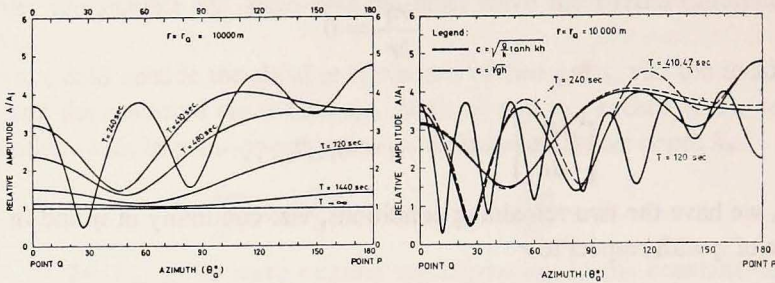$$\nabla \cdot (h\nabla\eta) + \frac{\omega^2}{g}\,\eta = 0 . \tag{3.18}$$

Figure 2. Relative amplitude A/A_i at shoreline vs. azimuth $\theta°_a$. (a) (left) Corresponding to an analytical shallow water diffraction solution. (b) (right) Corresponding to a numerical intermediate depth diffraction solution and two curves from (a).

For this case, Homma (1950) solved the infinite set of linear two-point boundary problems (3.9), (3.11), and (3.16). With our symbols Homma's solution reads

$$\frac{\eta}{A_i} = \sum_{n=0}^{\infty} \frac{\frac{2}{\pi} \epsilon_n i^{n+1} \rho \left[\left(\frac{r}{r_a}\right)^{-1+\alpha_n} + \frac{\alpha_n-1}{\alpha_n+1} \left(\frac{r}{r_a}\right)^{-1-\alpha_n} \right] \cos(n\theta)}{\rho^{\alpha_n}[(1-\alpha_n)H_n + \tau H'_n] + \rho^{-\alpha_n} \frac{\alpha_n-1}{\alpha_n+1} [\tau H'_n + (1+\alpha_n)H_n]}$$

(3.19)

where $\alpha_n \equiv \sqrt{1 + n^2 - \tau^2}$, $\rho \equiv r_b/r_a$ and we have dropped the argument τ of the Hankel function and its derivative.

Vastano and Reid (1967) presented the solution at the island boundary ($r = r_a$ in Fig. 1) in graphical form for one set of the geometrical constants, which define the island (their Table II). However, this table is a little confusing in two respects. Firstly, their Figs. 7-8 correspond in fact to shoreline radius $r_0 = 10.5$ km, and not to $r_0 = 10$ km as written in Table II. The correct value of r_0 was implied on p. 134 of their paper. The reason for using $r_0 = 10.5$ km in the analytical solution was simply to make a fair comparison with the numerical one, since the effective boundary in the numerical model is midway between the first two grid points. Secondly, their shoreline depth D_0 is in fact $4,000 \times (10.5/30)^2 = 490$ m, and not 400 m as stated in the table. (Nor does it correspond to $r_0 = 10$ km.) This was confirmed by Professor Reid (1973).

As Figs. 7 and 8 (relative amplitude and phase lag at the shoreline) in Vastano and Reid (1967) have been reproduced in other papers (Lautenbacher, 1970, p. 659; Berkhoff, 1973, pp. 485-486; and Shaw, 1974, p. 1358) it was found pertinent to publish similar figures, which really correspond to an inner radius of 10 km. These are reproduced in this paper in Figs. 2 and 3. The relevant geometrical data are given in Table 1. Note that Vastano and Reid (1967) only present results for $T = 240$ sec, 480 sec, and 720 sec.

Fig. 2a presents the relative amplitudes A/A_i at the island ($r = r_a$) versus azimuth $\theta°$, as defined in Fig. 1. On account of the symmetry only one half of the flow
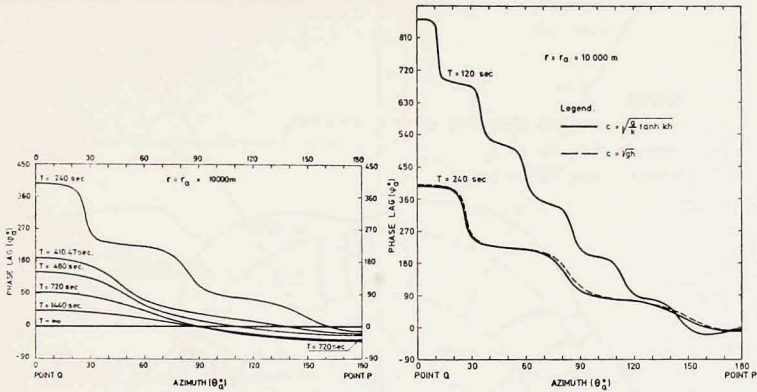
Figure 3. Phase lag $\phi°_a$ at shoreline vs. azimuth $\theta°_a$. (a) (left) Corresponding to an analytical shallow water diffraction solution. (b) (right) Corresponding to a numerical intermediate depth diffraction solution and a curve from (a).

plane is considered ($0° \leq \theta \leq 180°$). Note that the maximum amplitude does not necessarily occur for $\theta = 180°$ ($T = 410$ sec). The horizontal "wave length" of the undulations on the curves (fixed T) increases for increasing T. The "wave height" (fixed T) increases for decreasing T. As the fixed parameter for each curve one can instead of T use the relative wave length L_a/r_a ($= T\sqrt{g\alpha}$ for shallow water theory). As expected, A/A_i approaches 1 for all points along the circumference for $T \to \infty$ (a vertical staff in the ocean). However, the equations are not valid for such high values of T, as the Coriolis force cannot be neglected for T higher than (say) 30 min. From Fig. 7 we see that A/A_i still is 25% above the limiting value 1 for the highest value, where we can use the equations.

Fig. 3a presents the phase lag $\phi°$ versus azimuth $\theta°$. The angle ϕ is by definition the phase lag relative to the waves in the far field at $\theta = \pm 90°$, and it is identical with the phase lag in Vastano and Reid (1967), p. 131. (Note that point P at the middle of the front face of the island corresponds to $\theta = 180°$ and *not* to $\theta = 0°$.) So, if the far field at $\theta = \pm 90°$ is

$$\xi = A_i \exp(-i\omega t) \qquad (3.20)$$

then the amplitude at the shoreline is

$$\xi = A \exp[i (\phi - \omega t)] \qquad (3.21)$$

A being real amplitude. In Figs. 2a and 3a we have given the curves for 6 values of period T. The value of 410 sec (more accurately with 9 significant digits (9S): 410.471895 sec) corresponds to $h_b/L_b = 1/20$, using (2.1). So, for larger values of T, the shallow water wave assumption is justified in the whole area considered. The smallest period used in Figs. 2.a and 3.a ($T = 240$ sec) is thus, according to
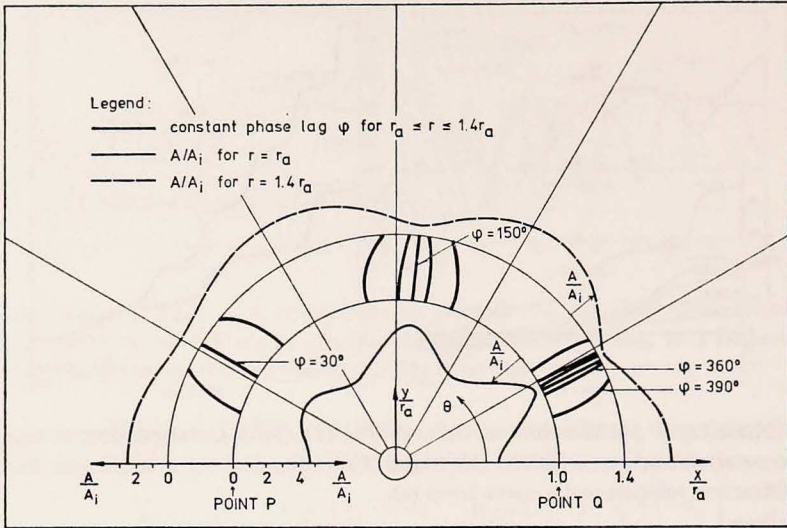
Figure 4. Constant phase lag curves $\phi°$ for $r_a \leqq r \leqq 1.4\, r_a$ vs. azimuth $\theta°$ corresponding to an analytical shallow water diffraction solution. $T = 240$ sec. The difference between the ϕ curves is 30°. Relative amplitude A/A_i at $r = r_a$ and $1.4\, r_a$ vs. azimuth $\theta°$.

normal conventions for h/L, too low; in this case, h_b/L_b is as high as $0.0883 \approx 1/11$. However, the shallow water solution for $T = 240$ sec is not dramatically off; see Figs. 2b, 3b, 5b, and 6. This is in accordance with the fact that the phase velocity for this period, as calculated from (2.2) is off by not more than 5% for $h = h_b$.

For a fixed time Fig. 4 depicts curves with constant phase lag ϕ for $r_a \leqq r \leqq 1.4$ r_a versus azimuth $\theta°$. The difference between the ϕ curves is 30°, and T is 240 sec. In the same figure also is given A/A_i at $r = r_a$ and $1.4\, r_a$ versus azimuth θ. We see that around a minimum in A/A_i the constant ϕ curves are relatively close, corresponding to a big gradient in ϕ. The reverse is the case around a maximum in A/A_i, i.e. a small gradient in ϕ. Comparing the situation around the minima we see that the smaller the minimum is, the greater is the gradient in ϕ.

In each point at the shoreline the curves corresponding to constant phase lag ϕ are perpendicular to the shoreline. If we, therefore, in each point decompose the calculated "wave" into two formal components, viz. an incident and a reflected component of equal amplitude, the angles α_1 between the propagation directions of the components and the normal to the shoreline are identical. As ϕ is known along the circumference, we can calculate a "local resulting phase velocity" c_{res} parallel to the shoreline as $\omega r_a/|d\phi_a/d\theta|$. If we determine the phase velocity of the incident and reflected component by (2.2), we then formally can define α_1 by arcsin $(\sqrt{gh_a}/c_{res})$, assuming that $c_{res} > \sqrt{gh_a}$ at least for certain parts of the circumference. From Fig. 4 we see that c_{res} has its maxima around the maxima of A/A_i
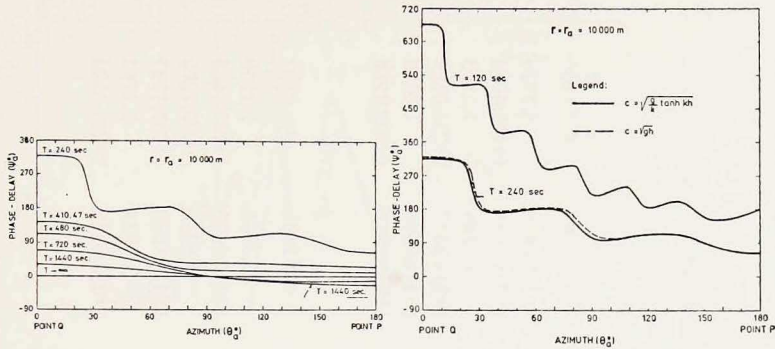
Figure 5. Phase delay $\psi°_a$ at shoreline vs. azimuth $\theta°_a$. (a) Corresponding to an analytical shallow water diffraction solution. (b) Corresponding to a numerical intermediate depth diffraction solution and a curve from (a).

($|d\phi_a/d\theta|$ small), i.e. α_1 has its minima at the maxima of A/A_i as would be expected intuitively. (See also the comments to Table 4 and Fig. 7 in Section 4.a.)

Figs. 3a and 3b depict the situation for a fixed time; the phase *lags* are so to speak simultaneous; see (3.20) and (3.21). However, for some considerations it might be more descriptive to study how much the wave at the island is delayed compared to the far field, for the same value of x (Fig. 1). In other words, the phase-*delay* (= "local phase lag") tells us how much the presence of the island (or more correctly: shoal plus island) has retarded the "undisturbed" wave field. This latter is, at the (imaginary) shoreline

$$\xi = A_i \exp[i(k_b r_a \cos(\theta_a) - \omega t)] \ . \tag{3.22}$$

From (3.21) and (3.22) it thus appears that the phase-delay at the shoreline is

$$\psi = \phi - k_b r_a \cos(\theta_a) \ . \tag{3.23}$$

The results are presented in Fig. 5.a. It is repeated that time is not constant along a $\psi(\theta)$-curve, in contrast to a $\phi(\theta)$-curve (Fig. 3).

In order to facilitate the checking of more general computer programs two numerical test solutions are tabulated in Table 2. In the table A/A_i and ϕ are given for two periods, for 7 values of θ, and for 3 values of r, viz. $T = 410.47$ sec (rounded $A_0 5S$) and $T = 120$ sec, $\theta = 0°$ (30°) 180°, and $r/r_a = 1$, 2 and 3. The values in Table 2.a are calculated using shallow water theory, and the values in Table 2.b are calculated using intermediate depth theory; see Section 3.b.

In this paper the comparison between a diffraction and a refraction solution will be made primarily for one point of the island, viz. for point P at the middle of the front face of the island, i.e. $\theta_a = 180°$. For waves below a certain period, part of the rear part of the island will be in a "geometrical shadow," and so a refraction solution will literally be one hundred percent wrong here. It is more difficult im-

Table 2. Diffraction solution for island on a paraboloidal shoal. The values of ϕ are chosen in the interval $0° \leqq \phi < 360°$. Integers in parentheses indicate powers of 10 by which the following numbers are to be multiplied.

(a) Using shallow water theory, $T = 410.47$ sec.

	$\theta = 0°$	$\theta = 30°$	$\theta = 60°$	$\theta = 90°$	$\theta = 120°$	$\theta = 150°$	$\theta = 180°$
$(A/A_i)_{r=r_a}$	3.2021	2.0974	2.0115	3.7047	4.0197	3.6878	3.5719
$(\phi°)_{r=r_a}$	(+2)1.8753	(+2)1.6778	(+1)7.3163	(+1)3.6224	(+1)1.3778	(+2)3.5138	(+2)3.4064
$(A/A_i)_{r=2r_a}$	2.2182	1.3142	1.2792	2.1593	1.7325	1.1709	1.1193
$(\phi°)_{r=2r_a}$	(+2)2.0852	(+2)1.8828	(+1)7.6237	(+1)4.0100	(+1)1.1791	(+2)3.3017	(+2)3.0684
$(A/A_i)_{r=3r_a}$	1.6998	(−1)8.8778	(−1)9.1434	1.1876	(−1)3.1524	(−1)7.8144	1.0058
$(\phi°)_{r=3r_a}$	(+2)2.3750	(+2)2.1720	(+1)8.1964	(+1)4.4105	(+2)3.3123	(+2)2.2010	(+2)2.0986

(b) Using intermediate depth theory, $T = 120$ sec.

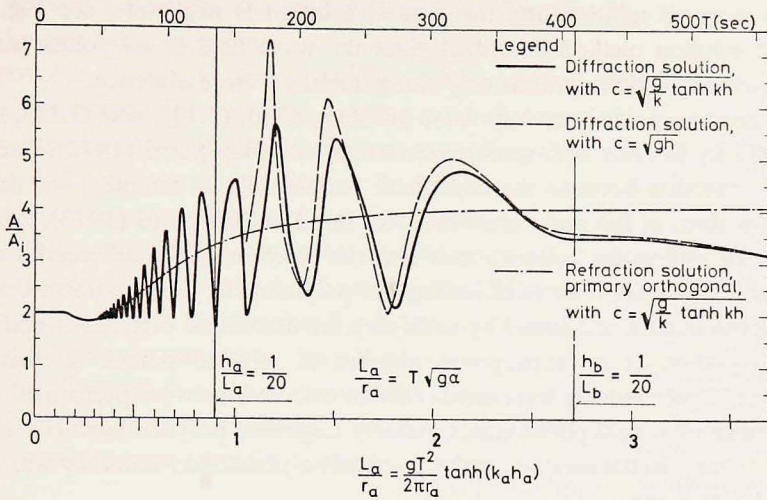|	$\theta = 0°$	$\theta = 30°$	$\theta = 60°$	$\theta = 90°$	$\theta = 120°$	$\theta = 150°$	$\theta = 180°$
$(A/A_i)_{r=r_a}$	3.6932	2.6044	1.1589	2.0652	2.4398	3.1314	2.1950
$(\phi°)_{r=r_a}$	(+2)1.4091	(+2)3.1459	(+1)7.3373	(+2)2.2080	(+1)9.2018	(+2)3.5820	(+2)3.5608
$(A/A_i)_{r=2r_a}$	(−1)1.1337	(−1)6.6582	1.7337	1.4507	(−1)2.2952	1.5422	(−1)6.7209
$(\phi°)_{r=2r_a}$	(+2)1.7030	(+2)1.2988	(+2)3.1049	(+2)1.3636	(+1)3.3566	(+1)1.8833	(+2)3.1337
$(A/A_i)_{r=3r_a}$	(−1)8.9702	(−1)6.9695	(−1)1.0274	1.6081	(−1)8.4291	1.1834	1.2761
$(\phi°)_{r=3r_a}$	(+2)1.1853	(+2)2.6433	(+1)5.4907	(+2)3.3509	(+2)1.0777	(+2)2.0168	(+2)1.8384

Figure 6. Relative amplitude A/A_i at point P ($\theta_a = 180°$) vs. wave period T and relative wave length L_a/r_a. Analytical shallow water diffraction solution, numerical intermediate depth diffraction solution, and numerical intermediate depth refraction solution for the primary orthogonal.

mediately to evaluate the error in the "illuminated zone". For one value of the wave period ($T = 410.47$ sec) we will also study the variation along the island circumference.

These comparisons are made in Figs. 6, 7, and 8, which will be discussed in detail in Section 3.b and Chapter 4. It should be noted that in Figs. 6 and 7 the amplitude varies rather rapidly with the wave period ("oscillates") when the wave length at the shoreline (L_a) becomes smaller than about the island diameter ($2r_a$). The "peaks" in this region correspond nearly to the island circumference, being an integer times the wave length at the shoreline. For the shallow water refraction solution this relation becomes exact, see Section 4.a. This effect cannot be detected from the figures by Vastano and Reid (1967), since they only consider the wave periods 240 sec, 480 sec, and 720 sec. The shallow water diffraction calculations are not pursued below $T = 160$ sec, since the shallow water approximation becomes increasingly inaccurate (as seen in Fig. 6). Using (2.1) we have that $h_a/L_a = 1/20$ corresponds to $T = 136.82$ sec. From Fig. 6 we conclude that the shallow water diffraction solution should not be used for $T \lesssim 300$ sec, or $L_a/r_a \lesssim 2$. For $T > 300$ sec the maximum error in peak amplitude at point P, using the shallow water diffraction solution, is only about 5%.

b. The diffraction solution using intermediate depth theory. This theory also covers periods below the normal tsunami range. We consider periods from (say) 1 sec to 1800 sec, but for (say) $L_a/r_a > 3.5$ or $T > 530$ sec the difference between

the shallow water solution and the general solution is negligible; see Fig. 6. The numerical solution method described gives the wave field in all points (see Table 2.b), but we will depict solutions only along the island circumference.

The linear two-point boundary value problem, (3.9), (3.11), and (3.16), is solved numerically by interior orthogonal collocation, see Skovgaard (1973), Sec. 4 and App. A. Note that because the dependent variable R_n is complex, we have used complex versions of the programs which are listed in Skovgaard (1973), App. A. A basic idea of orthogonal collocation is that the solution of the differential equation is represented by a finite series of orthogonal polynomials. The unknown coefficients in this representation are found by satisfying the associated conditions and the differential equation at an appropriate number of selected points. In this project shifted Jacobi polynomials were used. All the calculations were performed with the simplest form of Jacobi polynomials, namely Legendre polynomials. The necessary number of terms in the series in order to obtain a prescribed accuracy was decreasing with T increasing.

A finite number of solutions $R_n(r)$ $(n = 0,1,2, \ldots, n_{max})$ was then used to calculate η over the shoal (3.8)

$$\eta = \sum_{n=0}^{n_{max}} R_n(r)\cos(n\theta) . \tag{3.24}$$

The number n_{max} necessary to obtain a prescribed accuracy was decreasing for increasing period.

Figs. 2b, 3b, and 5b present A/A_i, ϕ, and ψ at the island ($r = r_a$) versus azimuth $\theta°$. The curves are similar to the corresponding ones in Figs. 2.a, 3.a, and 5.a. The amplitude A/A_i is given for three values of T (410.47, 240, and 120 sec), and ϕ and ψ are given for two values of T (240 and 120 sec). In the same figures are also given the curves corresponding to the analytical shallow water theory for $T = 410.47$ and 240 sec. For $T = 410.47$ sec the maximum difference between the two A/A_i curves is 4%, and for $T = 240$ sec it is 20%.

For point P the relative wave amplitude A/A_i is depicted in Fig. 6. For $L_a/r_a > 1.8$, or $T > 275$ sec, we see that the shallow water diffraction solution predicts higher values of A/A_i than does the diffraction solution using intermediate depth theory. The "peak values" predicted by the shallow water diffraction solution become increasingly too large for decreasing period.

Since the solution of (3.1) is more difficult than the solution of the long-wave equation (3.18), it would be useful if one could give the range of periods for which (3.1) must be used for an accurate estimate of the wave amplitude at the shoreline. However, only one island has been investigated here, and so general answers cannot be given. On the other hand, in the case of islands being similar to that in

Fig. 1, the conclusions for the periods found in Figs. 2b, 3b, 5b, and 6 may be extended, using Froudes scaling.

It is possible, though, to give an estimate of the smallest period, for which (3.18) suffices. If we accept that the water depth around ocean islands is seldom more than 4 km, the usually accepted (linear) shallow water limit $h/L = 1/20$ gives a limiting period of 410 sec, as stated in Section 3.a. So it can be expected that (3.18) will give a rather accurate estimate of the amplitudes for tsunami periods bigger than 7 min (with the reservation, naturally, that linear theory holds). This conclusion is substantiated by Figs. 2b and 6. (Summerfield, 1972, p. 362, proposes a shallow water condition, which implies that h_b/L_0 should be smaller than $1/(6\pi) \approx 1/19$, L_0 being the deep water wave length $gT^2/(2\pi)$. This condition corresponds to $h_b/L_b \lesssim 1/10$, which is a higher value than normally accepted. In the present case ($h_b = 4$ km) this gives $T > 220$ sec, and it turns out (see Figs. 2b and 6) that the errors in amplitude grow rapidly when we approach this limiting period.)

4. The refraction solution

Refraction theory for waves propagating over a varying sea bed is only applicable when the relative change in water depth is small over a wave length, i.e.

$$|\nabla h| \ll h/L \qquad (4.1)$$

since $|\nabla h|$ is the maximum bed slope. Using (2.2) for simplicity, we find the requirement for the present shoal to be

$$2T \sqrt{g\alpha} \ll 1 \ . \qquad (4.2)$$

For $T = 136$ sec ($h_a/L_a = 1/20$) we find $2T \sqrt{g\alpha} = 1.8$, and for $T = 410$ sec ($h_b/L_b = 1/20$) $2T \sqrt{g\alpha} = 5.4$. This shows that for the present shoal (4.1) is in fact only fulfilled for waves of rather small period. It can be shown, however, that in practice (4.1) need not be followed very strictly. Thus for plane waves it can be shown that the reflection coefficient (amplitude) will only be about 3% if $|dh/dx|$ equals h/L. So (4.1) might read "somewhat smaller than" instead of "much smaller than". We still have a dilemma here, though. Equation (4.1) requires T smaller than (say) 50 sec (see the end of this paragraph in connection with Fig. 6), while the shallow water theory used in the "complete" refraction solution (see later) requires T larger than (say) 400 sec. Fortunately, as it appears from Fig. 6, the difference between the shallow water and the true diffraction solution is not dramatic for $T \gtrsim 200$ sec. This makes it worth while to compare a shallow water refraction solution with a diffraction ditto in an (unspecified) range about 200 sec.

A more consistent evaluation of the refraction approximation can be made along the lines of Vastano and Reid (1966), pp. 37-38. They have omitted, though, the term $\nabla^2 A/A$ at the right-hand side of their equation (53).

The wave orthogonals are determined by three first-order ordinary differential equations, see e.g. Skovgaard *et al.* (1975), equations (2)-(4)

$$\frac{Dx}{Ds} = \cos v \tag{4.3}$$

$$\frac{Dy}{Ds} = \sin v \tag{4.4}$$

$$\frac{Dv}{Ds} = -\frac{1}{c}\frac{dc}{dh}\left(\frac{\partial h}{\partial x}\sin v - \frac{\partial h}{\partial y}\cos v\right) \tag{4.5}$$

where D = operator for differentiation along the wave orthogonal (s), and v = angle between x-axis and wave orthogonal (positive counterclockwise). For the present shoal we furthermore have

$$\frac{\partial h}{\partial x} = 2\alpha r \cos \theta \ (= 2\alpha x) \tag{4.6}$$

$$\frac{\partial h}{\partial y} = 2\alpha r \sin \theta \ (= 2\alpha y) \tag{4.7}$$

$$\frac{\partial^2 h}{\partial x^2} = \frac{\partial^2 h}{\partial y^2} = 2\alpha \tag{4.8}$$

$$\frac{\partial^2 h}{\partial x \partial y} = 0 \ . \tag{4.9}$$

After some trivial manipulation we get from (4.3)-(4.7)

$$\frac{Dv}{Ds} = \frac{2G}{1+G}\frac{D\theta}{Ds} \ . \tag{4.10}$$

The wave amplitude along an orthogonal can be calculated using the differential equation for the wave orthogonal separation factor β, derived by Munk and Arthur (1952). This equation reads

$$\frac{D^2\beta}{Ds^2} + p_s\frac{D\beta}{Ds} + q_s\beta = 0 \tag{4.11}$$

in which we for the present shoal have

$$p_s = -\frac{2}{r}\frac{G}{1+G}\cos (v-\theta) \tag{4.12}$$

$$q_s = \frac{2}{r^2}\frac{G}{1+G}\left[1 - \frac{4gh}{c^2(1+G)^2}\sin^2 (v-\theta)\right] \ . \tag{4.13}$$

The quantity β is defined as the distance between two neighboring orthogonals at an arbitrary point, divided by the corresponding distance at some initial point. The modified refraction coefficient therefore is

$$K'_{ra} = \beta^{-\frac{1}{2}} \tag{4.14}$$

see Skovgaard *et al.* (1975, 1976).

The initial values for (4.3)-(4.5) and (4.11) at the outer radius of the shoal are

$$r = r_b; \; \theta = \theta_b; \; v = 0; \; \beta = 1; \; D\beta/Ds = \kappa_{fb} \tag{4.15}$$

in which $90° < \theta_b < 270°$, and κ_{fb} is the curvature of the wave front for $r = r_b-$. From simple geometrical considerations we find, using also (4.10)

$$\kappa_{fb} = -\frac{2}{r_b} \frac{G}{1+G} \sin \theta_b \tan \theta_b \; . \tag{4.16}$$

Note, that the wave front curvature is discontinuous for $r = r_b$. For $r = r_b +$ we have $\kappa_{fb} = 0$ (plane incidence).

a. Refraction solution for shallow water waves. In this limit the phase velocity is determined by (2.2) and we have $G = 1$. The wave orthogonal direction is determined by (4.10), which now reads

$$\frac{D(v-\theta)}{Ds} = 0 \tag{4.17}$$

i.e. all orthogonals over the shoal are logarithmic spirals. This means that all incident orthogonals in the interval $-r_b < y < r_b$ will reach the shoreline sooner or later, some of them first having "whirled" many times around the island.

The orthogonals are independent of the wave period, being determined exclusively by θ_b. Using (4.15) the solution to (4.17) becomes

$$r = r_b \exp[(\theta_b - \theta) \cot \theta_b] \begin{cases} \theta < \theta_b \text{ for } 90° < \theta_b < 180° \\ \theta > \theta_b \text{ for } 180° < \theta_b < 270° \end{cases} \tag{4.18}$$

or

$$\theta = \theta_b - \ln(r/r_b) \tan(\theta_b) \qquad r_a \leqq r \leqq r_b \; . \tag{4.19}$$

Equations (4.18) and (4.19) do not give a unique solution for θ_b for a given set (r,θ). In fact, for every (r,θ) on the shoal there is an infinite number of roots θ_{bn} $(n = 1,2, \dots)$ in (4.18) or (4.19). This means that the (complex) amplitude everywhere is a sum of an infinite number of complex amplitudes, each one corresponding to its logarithmic spiral. The roots were found numerically, using the Newton-Raphson iterative method (see e.g. Hamming (1973), p. 68) which converges quadratically. A selection of roots is given in Table 3 for point P (Fig. 1). It appears that the spirals tend to lie infinitely close as θ_b tends to $90°+$ (or $270°-$). In the table, n is the number of the root. Every odd root (except the first one) is symmetrical with the preceding even one, i.e. $\theta_{b3} + \theta_{b2} = 360°$, $\theta_{b5} + \theta_{b4} = 360°$, etc., corresponding to spirals which are symmetrical about the x-axis. Observe that the roots are independent of T, in accordance with the spirals being independent of this quantity.

Table 3. Refraction solution (extract) for point P at the island (Figure 1) using shallow water wave theory. The two columns to the right correspond to $T = 410.47$ sec. Integers in parentheses indicate powers of 10 by which the following numbers are to be multiplied. The values of ϕ_n are chosen in the interval $0 \leqslant \phi_n < 360°$.

n	$\theta°_{bn}$	β	$2K'_s K'_{ra,n}$	$\phi°_n$	$A_i^{-1} \left\| \sum\limits_{j=1}^{n} A_j \exp(i\phi_j) \right\|$
1	(+2)1.8000	(−1)6.9954	4.1418	(+1)1.3100	4.1418
2	(+2)1.0256	8.0787	1.2188	(+2)2.8232	4.3013
4	(+1)9.5655	(+1)3.8045	(−1)5.6162	(+1)2.7953	5.1859
10	(+1)9.2106	(+2)2.7163	(−1)2.1019	7.5031	5.1356
100	(+1)9.0201	(+4)2.9648	(−2)2.0118	(+2)1.2653	5.1343
1000	(+1)9.0020	(+6)2.9916	(−3)2.0028	(+2)2.6082	5.1238

Since dissipation is neglected, the individual amplitudes A_n at the shoreline are determined from

$$\frac{A_n}{A_i} = K'_{ra,n} K'_s (1 + K_r) \tag{4.20}$$

in which the modified shoaling coefficient K'_s (see Skovgaard *et al.*, 1975, equation 28) and the reflection coefficient K_r are both independent of n, and are given by

$$K'_s = (h_b/h_a)^{\frac{1}{4}} = (r_b/r_a)^{\frac{1}{2}} \tag{4.21}$$

$$K_r = 1 . \tag{4.22}$$

Having found the paths of the orthogonals, $K'_{ra,n}$ can now be found, solving (4.11) for β_n and substituting the result into (4.14). Using from (4.17) and (4.15) that $v - \theta_n = -\theta_{bn}$, (4.11) becomes with $G = 1$ and $c = \sqrt{gh}$

$$r^2 \frac{d^2\beta}{dr^2} - r \frac{d\beta}{dr} + \beta = 0 \qquad r_a \leqslant r \leqslant r_b \tag{4.23}$$

since $dr = ds \cos \theta_{bn}$. This equation is of the Euler type. With the initial conditions for $r = r_b$, $\beta = 1$ and $d\beta/dr = -(1/r_b) \tan^2\theta_b$, see (4.15) and (4.16), the solution to (4.23) reads for the shoreline

$$\beta_n = \frac{r_a}{r_b} \left[1 - \ln \left(\frac{r_a}{r_b} \right) \sec^2\theta_{bn} \right] \tag{4.24}$$

where β_n ($n = 1, 2, \ldots$) corresponds to θ_{bn}. As θ_{bn} is independent of T, this applies also to β_n. Using (4.14) we therefore find

$$K'_{ra} = \left[\frac{r_a}{r_b} \left(1 - \ln \left(\frac{r_a}{r_b} \right) \sec^2 \theta_{bn} \right) \right]^{-\frac{1}{2}} . \tag{4.25}$$

It appears from the above development that in the shallow water limit, A_n/A_i only depends on which point of the shoreline we consider. So it is the differences in phase that make the resulting relative amplitude A/A_i at a fixed point a function
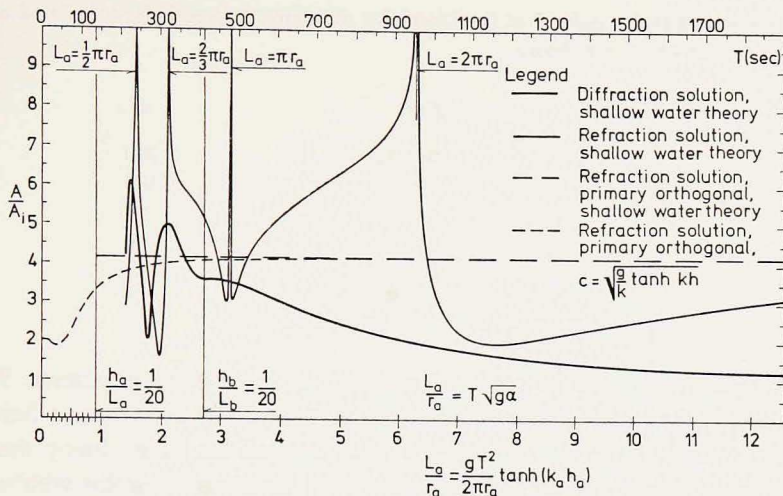
Figure 7. Relative amplitude A/A_i at point P vs. wave period T and relative wave length L_a/r_a. Analytical shallow water diffraction and refraction solutions, and numerical intermediate depth refraction solution for the primary orthogonal.

of period. Some examples are shown in Figs. 9-11. With the chosen definition of phase lag we find for the individual amplitude at the shoreline

$$\phi_n = \frac{\omega}{\sqrt{g\alpha}} \left[\cos\theta_{bn} + \frac{\ln(r_a/r_b)}{\cos\theta_{bn}} \right]. \tag{4.26}$$

The resulting relative shoreline wave amplitude is then

$$\frac{A}{A_i} = \left| \sum_{n=1}^{\infty} \frac{A_n}{A_i} \exp(i\phi_n) \right|. \tag{4.27}$$

A solution is given in Table 3 for point P. K'_s is constant along the shoreline and equal to $\sqrt{3}$ according to (4.21). The values of θ_{bn}, β and $2 K'_{ra,n}K'_s$ are independent of T for shallow water waves.

From Figs. 9 and 11 it is seen that after the summation of a certain number of terms on the right-hand side of (4.27), the sum becomes a damped oscillation. Therefore we did not develop a general criterion for determining the value of n_{max} at which the series (4.27) could be terminated. For each period a value for n_{max} was guessed, and if the sum for large n did not oscillate around one value, n_{max} was increased. Note that near the peaks, see Figs. 7 and 11, where n_{max} is of the order ten thousand, it is necessary to use a very high precision in the calculation of θ_{bn}. This is done in order to get a solution which for high values of n contains enough significant digits. Some of the calculations were done with 32 significant digits (32 S).

The relative wave amplitudes for point P are presented versus period in Fig. 7. The peak values are infinite for shallow water waves, and correspond to

Table 4. Phase angles for point P at the island for different peak periods, calculated according to shallow water refraction theory.

$p = \dfrac{2\pi\, r_a}{L_a}$	T sec	$\phi°$
1	951.72	270
2	475.86	180
3	317.24	90
4	237.93	0

$$\frac{2\pi r_a}{L_a} = p \qquad (p = 1,2, \ldots) \ . \tag{4.28}$$

The latter observation can be rendered probable in the following manner. We have seen previously that θ_{bn} is arbitrarily close to 90° (or 270°) except for a finite number. For n suitably large the orthogonals whirl around the island many times, and the logarithmic spiral can be approximated by a number of circles with a slowly decreasing diameter. Now, the interesting thing is that the time of travel t_s for a full circle is independent of the circle radius, since

$$t_s = \frac{2\pi r}{\sqrt{gh}} = \frac{2\pi}{\sqrt{g\alpha}} \qquad r_a \leq r \leq r_b \ . \tag{4.29}$$

Two neighboring orthogonals, which both reach the shoal for $x \approx 0$ (Fig. 1) and meet at the same point of the island, will therefore be nearly in phase at the shoreline and so amplify each other, if the travel time for one circle is a multiple of the period, i.e. if

$$\frac{2\pi}{T\sqrt{g\alpha}} = p \qquad (p = 1,2, \ldots) \ . \tag{4.30}$$

The left-hand side of (4.30) (which is recognized as the outer factor in (4.26)) is easily seen to be equal to the left-hand side of (4.28), so conditions (4.28) and (4.30) are in fact identical. This can also be shown analytically, since for large n the following expression is found for the phase lag of the individual amplitude at point P

$$\phi_n = \frac{\omega}{\sqrt{g\alpha}} \left(n\, 2\pi - \frac{\pi}{2} + 0(n^{-1}) \right) \tag{4.31}$$

so for p in (4.30) being an integer, the individual amplitudes tend to be in phase. It can also be shown that in this case the series (4.27) becomes divergent. This observation together with (4.31) furthermore shows that the phase lag for the resulting amplitude at point P is $p(-90°)$. This "phase lag limit" can also be found from a simple, geometrical consideration similar to that which led to condition (4.30). The predicted peak periods and the corresponding phase lags are given in Table 4. Note, though, that for p larger than (say) 2, the prediction becomes inaccurate because of the shallow water wave approximation. It is interesting to note
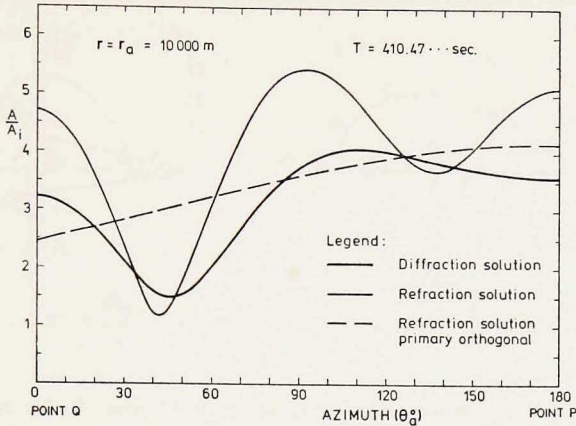
Figure 8. Relative amplitude A/A_i at shoreline vs. azimuth $\theta°_a$ for wave period $T = 410.47$ sec. Analytical shallow water diffraction and refraction solutions.

that the peaks in A/A_i (Fig. 7) at the "resonance" periods (Table 4, (4.28), and (4.30)) are located to the right of the corresponding peaks in the shallow water diffraction solution. Using this observation, and the fact that the "wave length" in the two solutions is identical, we have in the shallow water diffraction solution a mean c_{res} (see Section 3.a) which is greater than $\sqrt{gh_a}$. The agreement between the "resonance" periods is more significant for $p = 3$ ($T = 317.07$ and 317.24 sec) than for $p = 4$ ($T = 221.86$ and 237.93 sec) and is absent for $p = 1$ and 2. We remark that the "resonance" period for $p = 2$, which is absent in the shallow water theory diffraction solution, is present in the intermediate depth theory diffraction solution (just discernible in Fig. 6). Here too the diffraction "resonance" period $T = 450.38$ sec is smaller than the refraction "resonance" period $T = 475.86$ sec in Table 4.

Although the critical periods are rather well predicted for $p = 3$ and 4, the resulting wave amplitudes from shallow water wave refraction at these points have no connection with reality. The minimum refraction amplitudes come for some unknown reason close to the diffraction solution. The primary orthogonal ($A/A_1 = 4.1418$) is seen to give a poor representation of the complete refraction solution.

In Fig. 8 one of the shallow water diffraction solutions from Fig. 2a ($T = 410$ sec) is compared with the shallow water refraction solution. The undulations of the refraction curve are larger than those of the diffraction curve. The point where the relative amplitude has a minimum ($\theta_a \approx 45°$) is seen to be reasonably well predicted by the refraction solution. The primary orthogonal in the refraction solution gives only a "moving average" variation of A/A_i and thus cannot predict the more exposed regions of the shoreline of the island. Referring to Fig. 7 it can be seen that if in Fig. 8 we had chosen a period close to a peak value, the deviation from the diffraction curve would have been much larger.
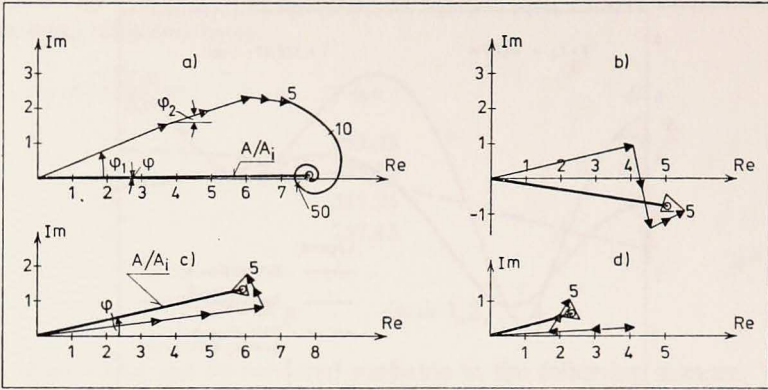
Figure 9. Vector addition of wave surface displacements at point P due to a shallow water refraction solution; (a) $T = 240$ sec, (b) $T = 410.47$ sec, (c) $T = 720$ sec, (d) $T = 1440$ sec.

Fig. 9 presents the vector addition of surface displacements in the complete refraction solution for point P due to shallow water waves. Four periods ($T = 240$, 410, 720, and 1440 sec) are considered. For the three latter values of T we come very close to the final magnitude of A/A_i after the addition of 5-10 orthogonals,
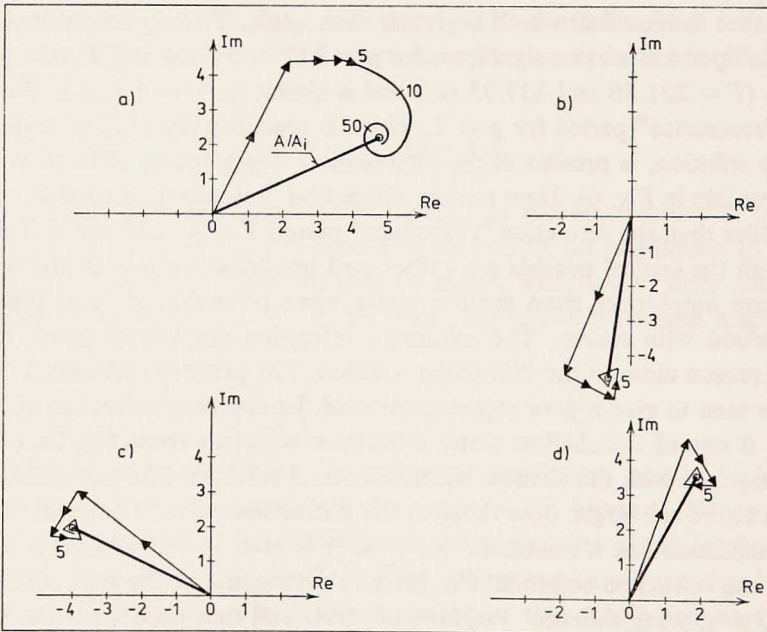

Figure 10. Vector addition of wave surface displacements at point Q ($\theta_a = 0°$) due to a shallow water refraction solution; (a) $T = 240$ sec, (b) $T = 410.47$ sec, (c) $T = 720$ sec, (d) $T = 1440$ sec.
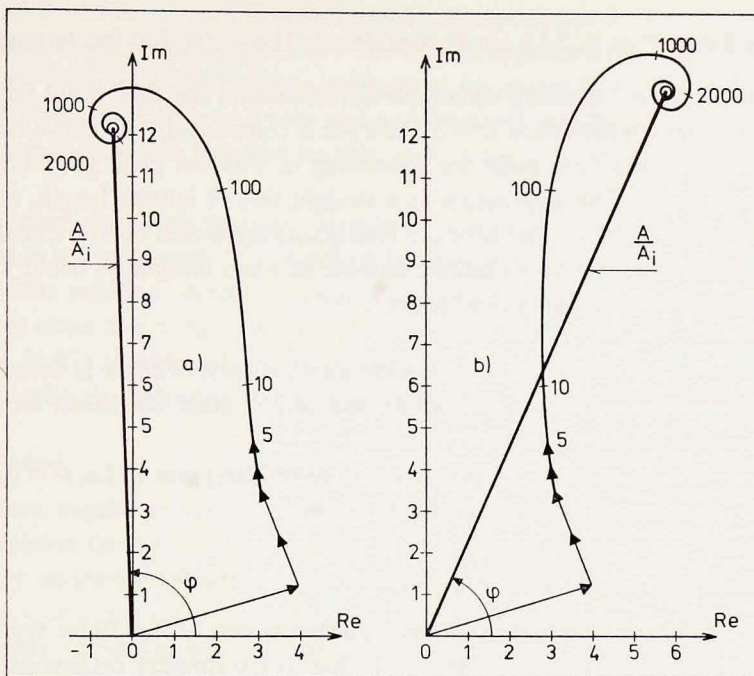
Figure 11. Vector addition of wave surface displacements at point P due to a shallow water refraction solution; (a) $T = 317.15$ sec, (b) $T = 317.30$ sec.

although we deal with an infinite (complex) series. For $T = 240$ sec, however, we need 50-100 orthogonals. This is because this period is close to a peak period $\approx$ 238 sec, see Table 4 and Fig. 7. For $T = 720$ sec the waves from the three first orthogonals are in phase, and the resulting A/A_i is rather high. For $T = 1440$ sec the waves from the second and third orthogonal are in opposite phase with the waves from the primary orthogonal, and the resulting A/A_i becomes rather low. Note, that the moduli in the four sets of vectors are the same, while the phase lags are different. It can also be seen that because of symmetry $(A_2,\phi_2) = (A_3,\phi_3)$, $(A_4,\phi_4) = (A_5,\phi_5)$, etc.

Fig. 10 is similar to Fig. 9 but depicts conditions for the opposite point of the island, point Q in Fig. 1. We remark that the first waves for $T = 720$ sec are not in phase as they were for point P, nor are the first waves for $T = 1440$ sec in opposite phase as they were for point P. For $T = 240$ sec we find the same tendency as in Fig. 9. This is so because the peak periods (but not the phase lags) are independent of θ_a. Note, that at point Q we have two equal primary orthogonals, two equal secondary orthogonals, etc.

Fig. 11 is a supplement to Fig. 9 (point P) showing two periods ($T = 317.15$ sec and 317.30 sec) on either side of the peak at $T = 317.24$ sec (Table 4). To the

left in the figure $T = 317.15$ sec is considered. The curve for the termini of $\sum_{j=1}^{j=n}$
$A_j/A_i\exp(i\phi_j)$ is here whirling counterclockwise around the final point for increasing n. To the right in the figure $T = 317.30$ sec is considered. The curve here whirls clockwise around the final point for increasing n. For the peak period itself, the curves would in the limit degenerate to a straight line of infinite length, and it can be inferred from the figure that here the final phase lag would be 90° (Table 4).

This method of adding up an infinite number of wave ortogonals could justify the name, a "vector addition refraction theory".

b. Refraction solution using intermediate depth theory. When c is determined by (2.1) the governing equations (4.3)-(4.5) and (4.11) must be solved numerically; see Skovgaard *et al.* (1975, 1976) for details.

Here we will only consider the primary orthogonal for point P, i.e. $\theta = \theta_b = 180°$ and $v = 0°$. In this case the equation for β simply is

$$\frac{1+G}{2G} x^2 \frac{d^2\beta}{dx^2} - x\frac{d\beta}{dx} + \beta = 0 \qquad -r_b \leq x \leq -r_a . \qquad (4.32)$$

In (4.32) G is a function of x, and the equation is not of the Euler type, as was (4.23). The relative wave amplitude A_1/A_i due to the primary orthogonal at point P becomes

$$\frac{A_1}{A_i} = 2\beta^{-\frac{1}{2}}_a \left[\frac{(1+G_b)\,c_b}{(1+G_a)\,c_a}\right]^{\frac{1}{2}} \qquad (4.33)$$

where factor 2 is due to the full reflection assumed. The value of A_1/A_i as a function of T is depicted in Figs. 6 and 7. For increasing T the curve approaches asymptotically the primary orthogonal solution from shallow water theory. For T smaller than about 25 sec, A_1/A_i is very close to 2.0 (fully reflected deep water waves). Now we know that for $T \to 0$ the orthogonals tend to become straight lines and in this limit every point of the "illuminated" part of the island ($90° \leq \theta \leq 180°$) will be reached by only one orthogonal (and the lee side by none at all). On the other hand, it was shown in the preceding section that in the shallow water limit every point is reached by an infinity of orthogonals. It therefore is expected that point P will be reached by $1,3,5, \ldots ,m, \ldots$ orthogonals for $0 < T < T_1$, $T_1 < T < T_2$, $T_2 < T < T_3, \ldots , T_{(m-1)/2} < T < T_{(m+1)/2}$, etc., where $m \to \infty$ for $T \to \infty$. Although this has not been investigated further (and thus we do not know when T_1 is reached and the primary orthogonal is no longer sufficient), it can be seen from Fig. 6 that this orthogonal with good accuracy gives a "moving average" of the true diffraction solution. And up to (say) $T \approx 50$ sec there is no real difference between the two solutions for point P. This can be taken as a "numerical proof" of the refraction theory being a limiting version of the wave equation. For $T = 50$ sec we find for the primary orthogonal along $\theta = 180°$, $|\nabla h|/(h/L) = 0.26$ for

$r = r_b$, and 0.58 for $r = r_a$. $|\nabla h|/(h/L) = 1$ corresponds to $T \approx 80$ sec for $r = r_a$ (where shallow water theory gives $T \approx 76$ sec). It appears from Fig. 6 that refraction theory, using only the primary orthogonal for point P, has broken down for this value of T. It might be a future task to investigate whether the inclusion of the omitted orthogonals will improve on this, and, if so, what the new limiting period would be.

In summary, the depth varying a significant amount over a distance that is small compared to a wave length is believed to be the major cause of the break-down of the refraction solution. Another contributing factor might be the discontinuity in the bottom slope at $r = r_b$. If we took into account the partial reflection here, then the series (4.27) would perhaps not diverge at the points in Fig. 7, and a better agreement with the diffraction solution might result.[4]

5. Conclusion

For plane, regular waves of small amplitude, incident on the island in Fig. 1, we have calculated the wave field according to two different approaches, viz. a diffraction theory and a depth refraction theory. The solutions are compared for periods where the Coriolis force can be neglected. It is found that for $1.5 \lesssim L_a/r_a \lesssim 2.5$ the complete refraction solution can predict the critical wave periods quite well, and to some extent also the regions of the shoreline where the wave amplitude is large. For L_a/r_a smaller than (say) 0.4, corresponding to rather small periods, Fig. 6, the amplitudes at point P (the middle of the front face of the island) are rather well predicted by the primary orthogonal. For L_a/r_a higher than this value the amplitudes from refraction theory deviate more and more from the diffraction solution. The primary orthogonal, however, can give the right order of magnitude for the wave amplitude in point P in the sense that it yields a good approximation to a "moving average" amplitude versus period diffraction curve up to $L_a/r_a \approx 2.5$. It cannot in any case predict the critical wave periods, nor the regions of the shoreline where the amplitude is large. Beyond $L_a \approx 2.5 \ r_a$ refraction calculations become quite meaningless. The complete refraction solution (i.e. superposing contributions from all orthogonals) is only calculated for shallow water waves.

The conflicting data in the definition of a similar island in Vastano and Reid (1966, 1967) are clarified. For another set of data the diffraction solution is given with a more complete description of the wave field over the shoal, and two test solutions are tabulated (Table 2).

The shallow water diffraction approach should not be used for L_a/r_a less than (say) 2 for the present island/shoal. For the first time the diffraction solution is given for an island of this form, using intermediate depth theory and a newly developed mild-slope wave equation. Generally, this equation may be replaced by

the well-known linear long-wave equation for tsunami periods bigger than 7 min. All nonliner effects have been neglected.

APPENDIX A: Calculation of the Bessel functions

The Bessel functions $J(x)$ and $Y(x)$ of order 0 and 1 were calculated from Chebyshev expansions, see Clenshaw (1962) and Luke (1969). For higher orders $J_n(x)$ were calculated by the forward recurrence relation for orders $n \leqq x$, see Olver (1964), equation (9.1.27). For orders n greater than x, $J_n(x)$ were calculated by a continued fraction, see Blanch (1964). For all orders n higher than 2, $Y_n(x)$ were calculated by the forward recurrence relation.

APPENDIX B: Programming

The numerical methods described were programmed in the IBM OS 360/370 implementation of PL/I. All the floating point calculations were made with at least 15S. All the presented results (Tables 2-4) were rounded to 5S.

REFERENCES

Arthur, R. S. 1946. Refraction of water waves by islands and shoals with circular bottom-contours. Trans. Am. Geoph. Union, *27*, 168–177.

Berkhoff, J. C. W. 1973. Computation of combined refraction-diffraction. Proc. 13th Coastal Engrg. Conf., July 1972, Vancouver, Chapter 24. New York, Am. Soc. Civ. Engrs., *1*, 471–490.

—— 1975. Linear wave propagation problems and the finite element method, *in* Finite Elements in Fluids. R. H. Gallagher, J. T. Oden, C. Taylor, and O. C. Zienkiewicz, eds. London, Wiley, *1*, 251–264.

Blanch, G. 1964. Numerical evaluation of continued fractions. Siam Review, *6*, 383–421.

Chen, H. S., and C. C. Mei. 1974. Oscillations and wave forces in an offshore harbor: Applications of hybrid finite element method to water-wave scattering. Ralph M. Parsons Laboratory for Water Resources and Hydrodynamics, Mass. Inst. Tech., Rep. No. 190, 215 pp.

Christiansen, P. L. 1975. Diffraction of gravity waves by large islands. Proc. 14th Coastal Engrg. Conf., June 1974, Copenhagen, Chapter 34. New York, Am. Soc. Civ. Engrs., *1*, 601–614.

Clenshaw, C. W. 1962. Chebyshev series for mathematical functions. Nat. Phy. Lab., Math. Tables. London, H.M.S.O., *5*, 36 pp.

Erdélyi, A., W. Magnus, F. Oberhettinger, and F. G. Tricomi. 1953. Higher transcendental functions. *II.* New York, McGraw-Hill, 396 pp.

Hamming, R. W. 1973. Numerical methods for scientists and engineers, 2nd ed. New York, McGraw-Hill, 721 pp.

Homma, S. 1950. On the behaviour of seismic sea waves around circular island. Geoph. Mag., *21*, 199–208.

Jonsson, I. G. 1967. Wave boundary layers and friction factors. Proc. 10th Conf. Coastal Engrg., Sep. 1966, Tokyo, Chapter 10. New York, Am. Soc. Civ. Engrs., *1*, 127–148.

—— 1975. The wave friction factor revisited. Inst. Hydrodyn. and Hydraulic Engrg. (ISVA), Tech. Univ. Denmark, Progr. Rep. No. 37, 3–8.

—— 1976. Discussion of: Friction factor under oscillatory waves, by J. William Kamphuis. Proc. Am. Soc. Civ. Engrs., J. Waterways, Harbors and Coastal Engrg. Div., *102* (WW1), 108–109.

Jonsson, I. G., and O. Brink-Kjaer. 1973. A comparison between two reduced wave equations for gradually varying depth. Inst. Hydrodyn. and Hydraulic Engrg. (ISVA), Tech. Univ. Denmark, Progr. Rep. No. 31, 13–18.

Jonsson, I. G., and N. A. Carlsen. 1976. Experimental and theoretical investigations in an oscillatory rough turbulent boundary layer. J. Hydr. Res., *14*, 45–60.

Kajiura, K. 1964. On the bottom friction in an oscillatory current. Bull. Earthquake Res. Inst., Univ. Tokyo, *42*, 147–174.

Keller, J. B. 1962. Geometrical theory of diffraction. J. Opt. Soc. Am., *52*, 116–130.

Larsen, J., and P. L. Christiansen. 1975. Computations of harbor oscillations by ray methods. Proc. Symp. on Modeling Techniques, San Francisco, Sep. 1975. New York, Am. Soc. Civ. Engrs., *2*, 888–906.

Lautenbacher, C. C. 1970. Gravity wave refraction by islands. J. Fluid Mech., *41*, 655–672.

Luke, Y. L. 1969. The special functions and their approximations. *II*. New York, Academic Press, 485 pp.

Madsen, O. S., and C. C. Mei. 1969. The transformation of a solitary wave over an uneven bottom. J. Fluid Mech., *39*, 781–791.

Meyer, R. E. 1971. Resonance of unbounded water bodies, *in* Mathematical Problems in the Geophysical Sciences. W. H. Reid, ed. Am. Math. Soc., Lect. in Appl. Math., *13*, 189–227.

Munk, W. H., and R. S. Arthur. 1952. Wave intensity along a refracted ray. Gravity Waves, Nat. Bur. Stds. Circular 521, Wash., D.C., U.S. Gov. Print. Off., Nov. 1952, 95–109.

Olver, F. W. J. 1964. Bessel functions of integer order, *in* Handbook of Mathematical Functions with Formulas, Graphs, and Mathematical Tables. M. Abramowitz, and I. A. Stegun, eds. Nat. Bur. Stds., Appl. Math. Ser., No. 55. Wash., D.C., U.S. Gov. Print. Off. 1046 pp.

Pocinski, L. S. 1950. The application of conformal transformations to ocean wave refraction problems. Trans. Am. Geoph. Union, *31*, 856–866.

Reid, R. O. 1973. Private communication. Nov. 1973.

Shaw, R. P. 1974. Time-harmonic wave scattering by obstacles in an infinite inhomogeneous medium. J. Acoust. Soc. Am., *56*, 1354–1360.

—— 1975. An outer boundary integral equation applied to transient wave scattering in an inhomogeneous medium. J. Appl. Mech., *42*, Trans. ASME, *97*, Ser. E, 147–152.

Skovgaard, O. 1973. Selected numerical approximation methods. Danish Center for Appl. Math. and Mech. (DCAMM), Rep. No. 62, Tech. Univ. Denmark. 71 pp.

Skovgaard, O., and J. A. Bertelsen. 1974. Refraction computations for practical applications. Proc. Int. Symp. on Ocean Wave Measurement and Analysis, New Orleans, Sep. 1974. New York, Am. Soc. Civ. Engrs., *1*, 761–773.

Skovgaard, O., I. G. Jonsson, and J. A. Bertelsen. 1975. Computation of wave heights due to refraction and friction. Proc. Am. Soc. Civ. Engrs., J. Waterways, Harbors and Coastal Engrg. Div., *101* (WW1), 15–32.

—— 1976. Closure to "Computation of wave heights due to refraction and friction." Proc. Am. Soc. Civ. Engrs., J. Waterways, Harbors and Coastal Engrg. Div., *102* (WW1), 100–105.

Smith, R., and T. Sprinks. 1975. Scattering of surface waves by a conical island. J. Fluid Mech., *72*, 373–384.

Sommerfeld, A. 1964. Partial differential equations in physics. Lectures on theoretical physics. New York, Academic Press, *6*, 335 pp.

Summerfield, W. 1972. Circular islands as resonators of long-wave energy. Phil. Trans. Roy. Soc. London, A, *272*, 361–402.

Svendsen, I. A. 1967. The wave equation for gravity waves in water of gradually varying depth. Coastal Engrg. Lab. and Hydraulic Lab., Tech. Univ. Denmark, Progr. Rep. No. 15, 2–7.

Svendsen, I. A., and I. G. Jonsson. 1976. A new wave equation for waves over a gently sloping sea bed. To be submitted for publication.

Vastano, A. C., and R. O. Reid. 1966. A numerical study of the tsunami response at an island. Dept. of Oceanography, Texas A & M Univ., A & M Project 471, Ref. 66-26T, 141 pp.

—— 1967. Tsunami response for islands: Verification of a numerical procedure. J. Mar. Res., *25*, 129–139.

CORRECTION
in

"The density of seawater solutions at one atmosphere as a function of temperature and salinity," by Frank J. Millero, Agustin Gonzalez and Gary K. Ward, J. Mar. Res., *34*, 61–93.

The values of $S(‰)$ and R_{15} given in Table 3 are incorrect. The correct values are given below:

0°C		25°C	
$S(‰)$	R_{15}	$S(‰)$	R_{15}
40.447	1.13752	40.049	1.12757
37.675	1.06791	36.944	1.04943
35.012	1.00030	35.137	1.00350
30.221	0.87673	29.772	0.86502
25.973	0.76482	25.647	0.75614
25.249	0.74551	24.730	0.73162
19.998	0.60317	19.632	0.59310
14.424	0.44731	14.408	0.44685
6.940	0.22775	6.613	0.21777
3.338	0.11462	3.017	0.10412
1.400	0.04975	1.306	0.04650

These corrections were unfortunately not made in the revised manuscript: 23 October, 1975. The correct salinities were used in all the density fits, thus equation (11) does not need to be altered.